

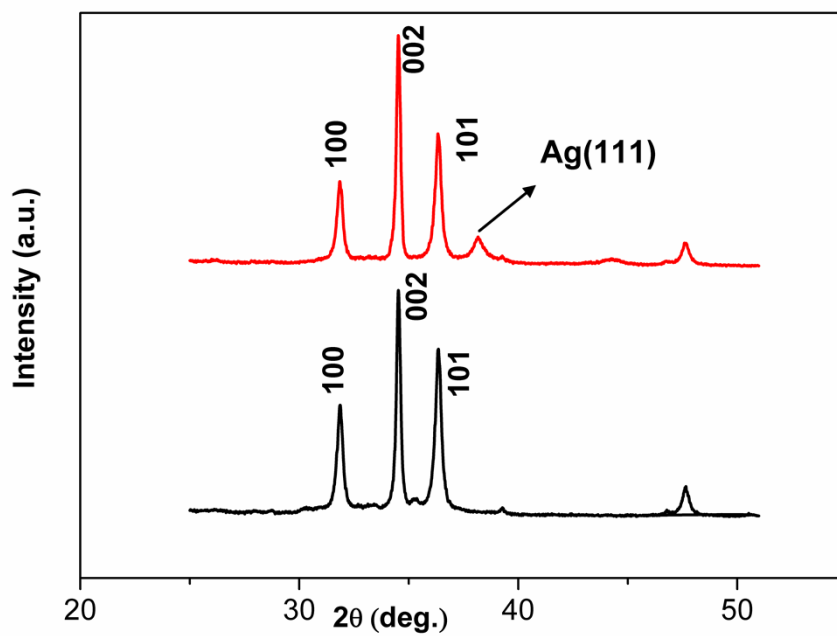
Supporting Information

Instruments

The as-prepared nanostructures on the substrate were sent to characterizations on a CAMSCAN APOLLO 300 field-emission scanning electron microscopy (FE-SEM) at 15KV. The crystal structure of the products was studied using a Bruker D8 X-ray diffractometer with Cu K α irradiation at $\lambda = 1.5406 \text{ \AA}$. For high-resolution TEM measurements, one drop of the alcohol dispersed suspension of sample was placed on a carbon-coated copper grid and allowed to dry in air. The grid was then observed on a Tecnai GF2 operated at an accelerating voltage of 400 kV. Selected area electron diffraction (SAED) patterns were also obtained. The absorbance spectrum of ZnO and ZnO-Ag hybrids samples were measured using a PerkinElmer Lambda35 fiber-optic UV-vis NIR spectrophotometer.

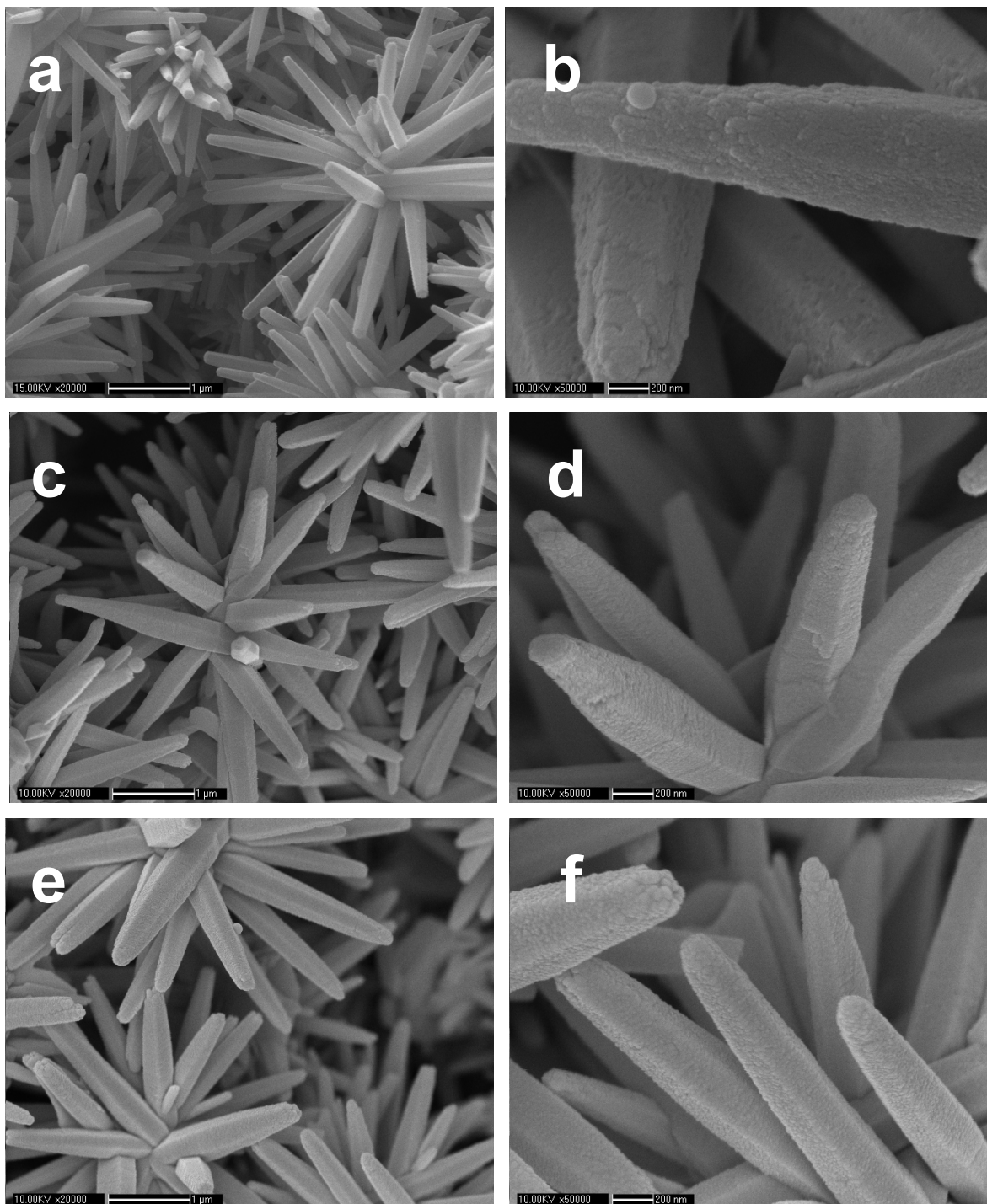
XRD experiments

Figure S1. XRD patterns of the flower-like ZnO nanostructure (the black line) and the flower-like ZnO-Ag hybrids (the red line).



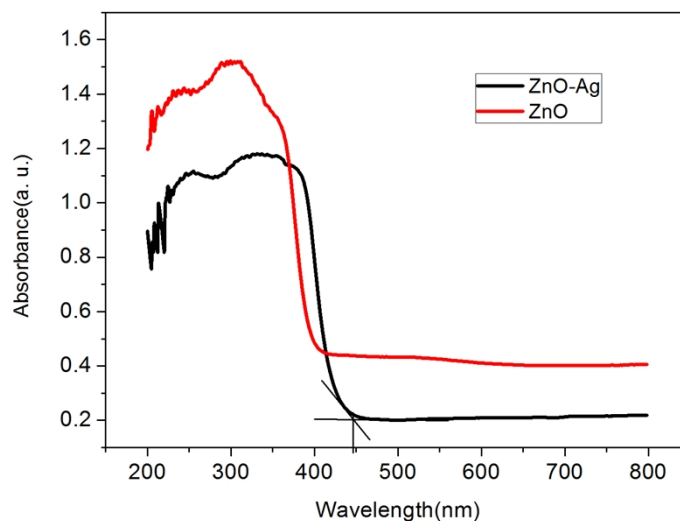
SEM Measurements

Figure S2. FE-SEM image of ZnO-Ag hybrids with different Ag deposition times, (a-b) 4min, (c-d) 16min, (e-f) 26min.



UV-vis experiments

Figure S3. UV-vis analysis of ZnO and ZnO-Ag substrate.



SERS experiments

Figure S4. The SERS spectra of R6G collected on the substrates with different Ag-sputtering durations exposed to a 1×10^{-8} M R6G solution with a data acquisition time of 5s.

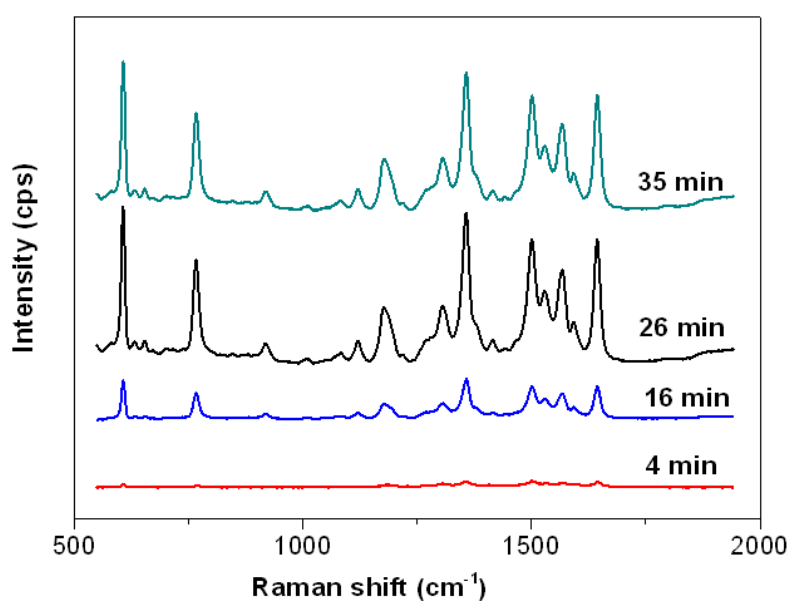


Figure S5. The SERS spectra of R6G collected on the ZnO-Ag hybrid substrate and Ag NPs substrate with the same Ag-sputtering time at 26 min, respectively; the data acquisition time was 5s.

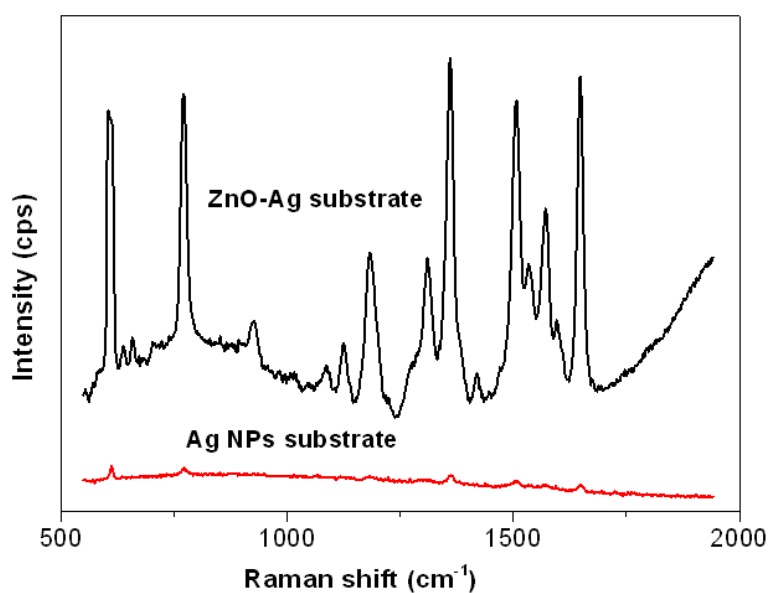


Figure S6. The SERS spectra of R6G collected on the ZnO-Ag substrates with different concentration of R6G 1×10^{-11} M to 1×10^{-12} M.

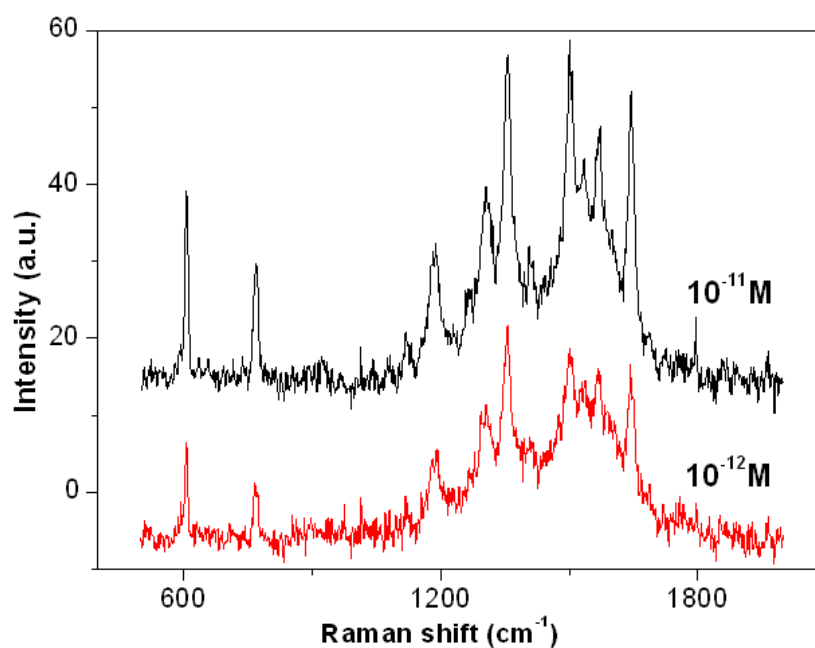
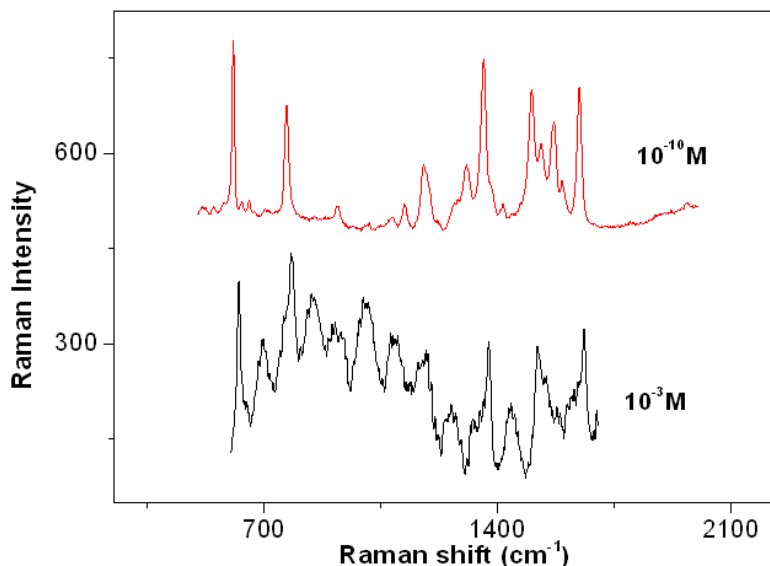


Figure S7. The Raman spectra of R6G with different concentration (1) collected on the ZnO-Ag substrates of 1×10^{-10} M and (2) collected on the Si-wafer with concentration of R6G at 1×10^{-3} M for comparison.



Estimation of enhancement factor

We use the peak at 611 cm^{-1} (for R6G) to estimate the enhancement factor (EF). The SERS EF is a quantitative measure of the Raman signal amplification of an analyte. We calculated this value using the reported protocol.^[1] The EF can be calculated by:

$$EF = \frac{I_{SERS} N_{Ref}}{I_{Ref} N_{SERS}}$$

Where N_{SERS} and N_{Ref} are the number of molecules probed on the nanoflower and on the reference sample, respectively. I_{SERS} and I_{Ref} correspond to SERS signal and the un-enhanced normal signals intensities, respectively. Herein, a certain volume (V_{SERS}) and concentration (C_{SERS}) R6G aqueous solution was dispersed to an area of Raman concentration for non-SERS Raman spectra certain S_{SERS} at the ZnO-Ag hybrid substrate. For non-SERS Raman spectra, a certain volume (V_{Ref}) and concentration (C_{Ref}) R6G

aqueous solution was dispersed to an area of S_{Ref} at a clean Si substrate. Both the substrates are dried in the air. Considering the area of laser spot is the same, the foregoing equation thus becomes:

$$EF = \frac{I_{SERS}}{I_{Ref}} \cdot \frac{C_{Ref} V_{Ref}}{C_{SERS} V_{SERS}} \cdot \frac{S_{SERS}}{S_{Ref}}$$

In our experiment, 1 μ L of 1×10^{-10} M R6G solution was dispersed to an area of 10 mm² for the ZnO-Ag hybrid substrate shown in Figure 2a and 1 μ L of 1×10^{-3} M R6G ethanol solution is dispersed to an area of π mm² for the silicon wafer. For the band at 611 cm⁻¹, I_{SERS}/I_{Ref} is 196/180=1.09. Therefore average enhancement factor for the band at 611 cm⁻¹ is calculated to be 4.12×10^6 . With the same method, the Efs for the SERS substrates shown in Figure 2a are estimated to be 4.12×10^6 .

Table S1. EF values estimated by different Raman bands in Figure 2a($C_{RS}=1 \times 10^{-3}$ M).

Raman band (cm ⁻¹)	C_{SERS} (M)	I_{SERS}/I_{RS}	EF	C_{SERS} (M)	I_{SERS}/I_{RS}	EF
611	1×10^{-10} M	1.09	4.12×10^6	1×10^{-9} M	1.16	4.39×10^6
771		1.01	3.82×10^6		0.94	3.56×10^6
1360		1.04	3.94×10^6		1.11	4.20×10^6
1649		0.92	3.48×10^6		1.04	3.94×10^6

Table S2. EF values estimated by different Raman bands of different substrates from different batch ($C_{RS}=1 \times 10^{-3}$ M).

Raman band (611 cm ⁻¹)	C_{SERS} (M)	I_{SERS}/I_{RS}	AEF
Substrate 1	1×10^{-10} M	0.94	3.56×10^6
Substrate 2		1.02	3.86×10^6
Substrate 3		1.12	4.24×10^6
Substrate 4		1.06	4.01×10^6

Figure S8. The corresponding RSD value curve.

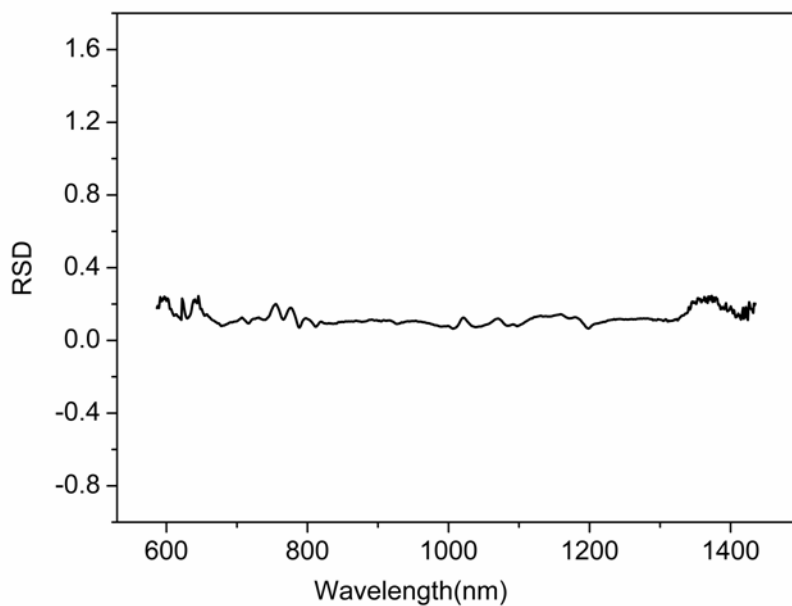


Table S3 RSD value of the major R6G characteristic SERS peaks

Peak position (cm ⁻¹)	611	771	1181	1360	1508	1572	1649
RSD value	0.13	0.16	0.13	0.21	0.14	0.22	0.18

Figure S9. The SERS spectra of 4-ATP collected on the ZnO-Ag hybrid substrates with Ag-sputtering for 26 min after being exposed to different concentrations of 4-ATP alcohol solution; the data acquisition time was 5s.

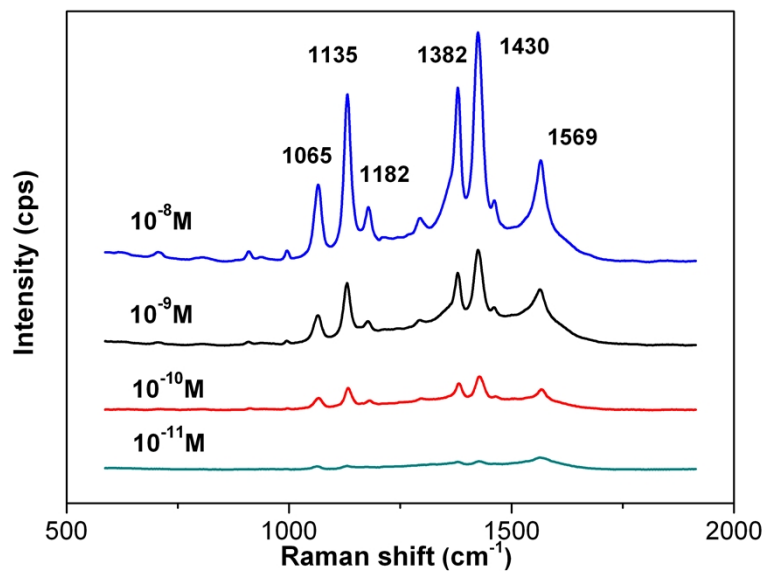


Figure S10. A series of SERS spectra of 4-ATP molecules collected on randomly selected 15 places of the ZnO-Ag hybrids substrate.

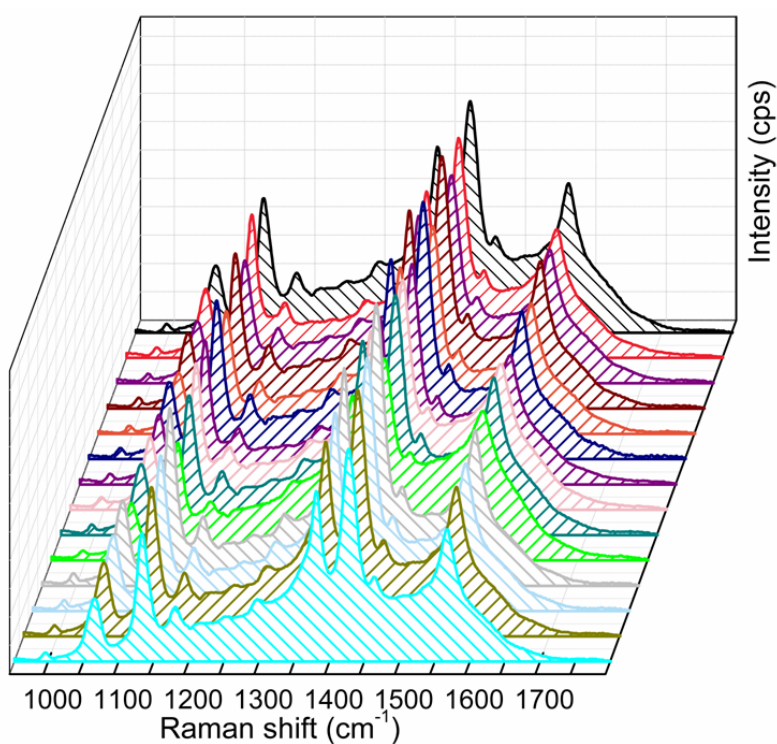
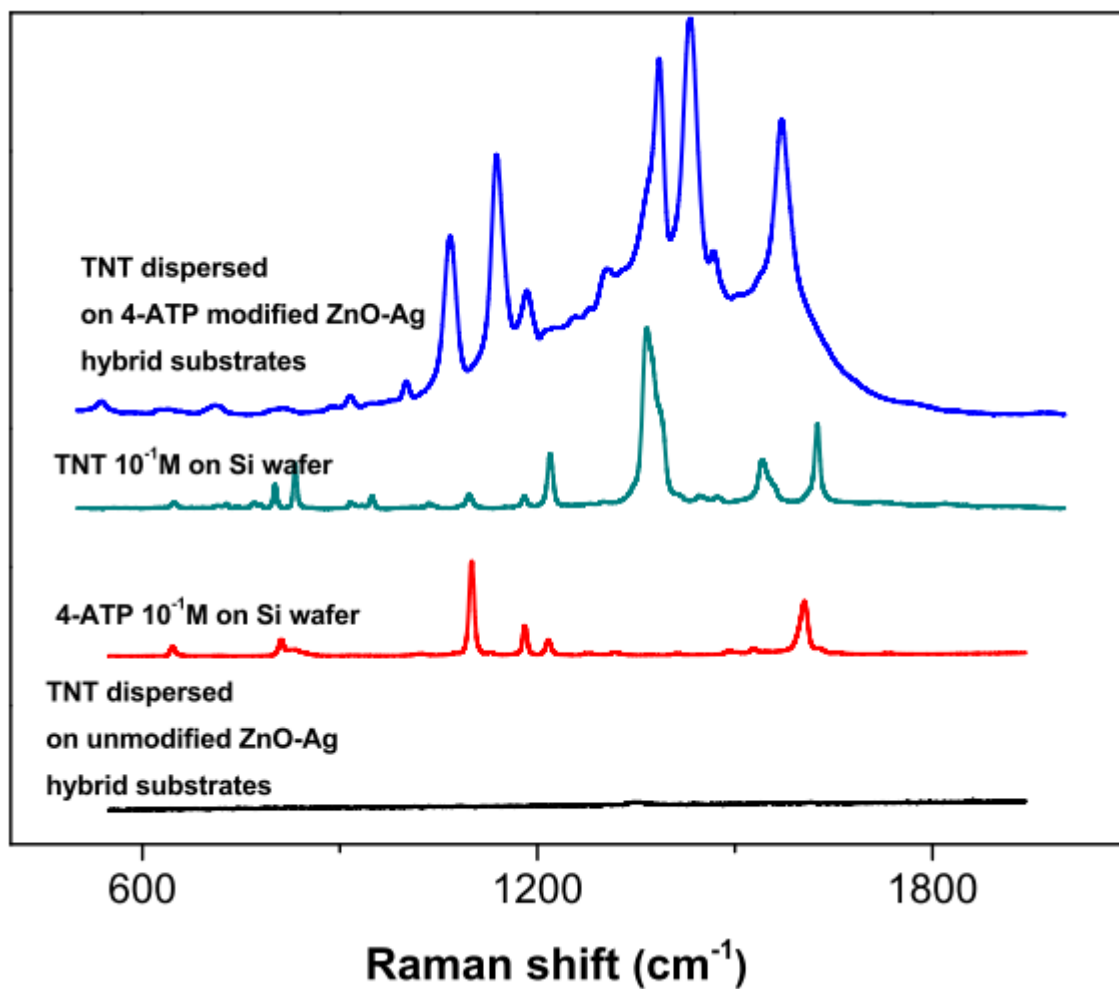


Figure S11. Pure TNT and pure 4-ATP on a blank substrate (Si wafer), and 10^{-6} M TNT (dissolved in ethanol) dispersed on unmodified or 4-ATP-modified ZnO–Ag hybrid substrates. The data acquisition time was 5s.



Calculation of frequency and Raman vibrational description

Figure S12. Vibrational mode of 4-ATP.

At the same level of theory, the frequencies and Raman intensities were calculated at the optimized geometry. The band at 1578 cm^{-1} due to the C-C ring stretching and 1079 cm^{-1} due to the C-S ring stretching was significantly enhanced. However, in our interpretation of the enhanced SERS bands of chemisorbed species, the Raman bands at 1569 cm^{-1} , allocated to stretching modes involving C-S bonds, were shifted to 1065 cm^{-1} . This shift might depend on the direction of the local electrical field at the molecular adsorption site and the molecular orientation with respect to the nanostructure surface.

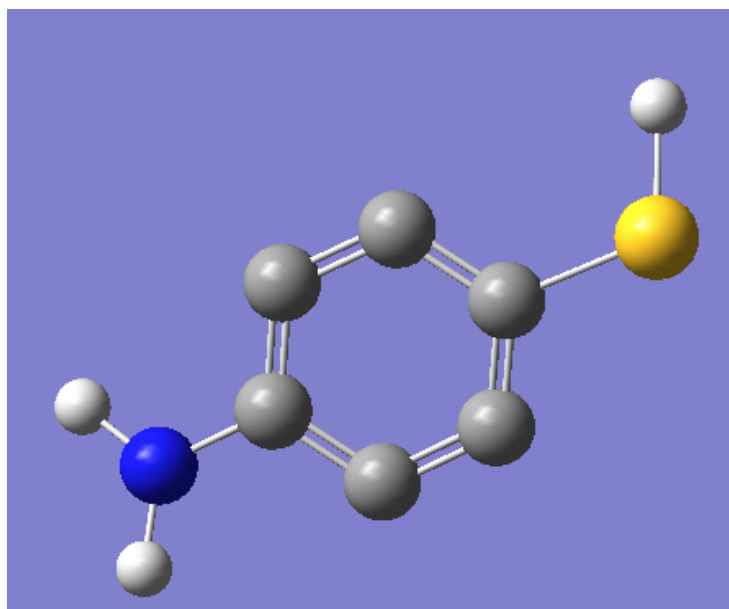


Table S4 Assignment of SERS and the vibrational description for 4-ATP^[2]

Vibrational description	SERS assignment
$\nu(\text{CC})$ ^[a]	1569
$\nu(\text{CS})$	1065
$\nu(\text{CC}) + \delta(\text{CH})$	1434
$\delta(\text{CH})$	1135

[a] ν , stretching; [b] δ , bending.

Figure S13. Vibrational mode of TNT

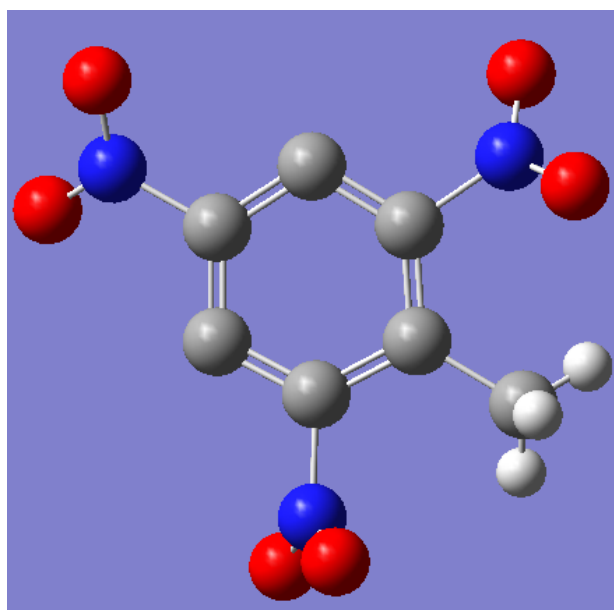


Table S5 Assignment of SERS and the vibrational description for TNT ^{[6][7]}

Vibrational description	SERS assignment
$\nu(\text{NO}_2)$ [a]	1365
$\nu(\text{C}=\text{C})$ ring	1616
$\delta(\text{CH})$ ring [b] + $\nu(\text{C}-\text{C})$	1167
$\delta(\text{CH})$ ring	1206
$\nu(\text{NO}_2)$	1527

[a] ν , stretching; [b] δ , bending.

Figure S14. (1) 10^{-6} M TNT (dissolved in ethanol) dispersed on 4-ATP-modified ZnO–Ag hybrid substrates; (2) 10^{-8} M 4-ATP-modified ZnO–Ag hybrid substrates; (3) Pure 4-ATP on a blank substrate (Si wafer), The data acquisition time was 5s.

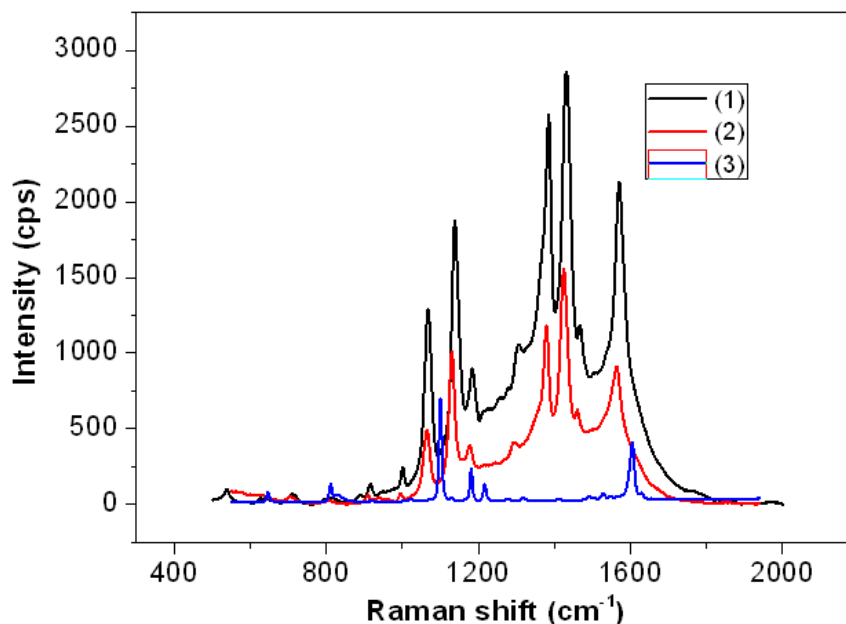
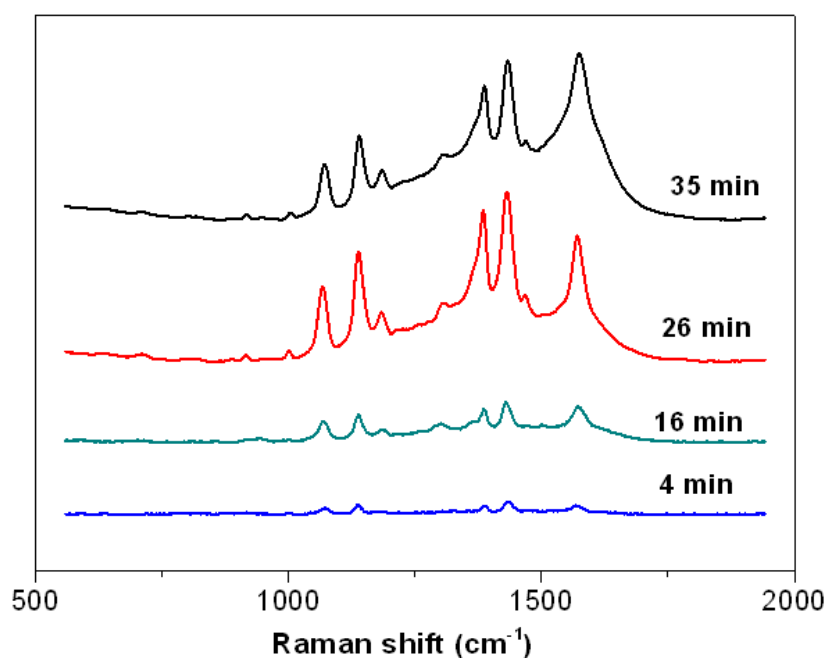


Figure S15. The SERS spectra of 4-ATP-functionalized ZnO-Ag hybrids with the presence of TNT(1×10^{-8} M) collected on the substrates with different Ag-sputtering durations exposed with a data acquisition time of 5s.



Besides, 4-ATP-functionalized ZnO-Ag hybrids with the presence of TNT(1×10^{-8} M) collected on the substrates with different Ag-sputtering durations at 4min, 16min, 26min,

and 35min, respectively. As shown in this figure, the 26min Ag-sputtering durations exhibited as the optimize time for composing ZnO-Ag hybrids substrate to TNT detection.

Reference

- [1] Z. Huang, G. Meng, Q. Huang, Y. Yang, C. Zhu and C. Tang, *Adv. Mater.* **2010**, *22*, 4136.
- [2] M. Osawa, N. Matsuda, K. Yoshii, I. Uchida, *J. Phys. Chem.* **1994**, *98*, 12702.